A new proofreading mechanism for lesion bypass by DNA polymerase-

Crespan, Emmanuele ; Maga, Giovanni ; Hübscher, Ulrich

Abstract: Replicative DNA polymerases (DNA pols) increase their fidelity by removing misincorporated nucleotides with their 3' → 5' exonuclease activity. Exonuclease activity reduces translesion synthesis (TLS) efficiency and TLS DNA pols lack 3' → 5' exonuclease activity. Here we show that physiological concentrations of pyrophosphate (PP(i)) activate the pyrophosphorolytic activity by DNA pol- , allowing the preferential excision of the incorrectly incorporated A opposite a 7,8-dihydro-8-oxoguanine lesion, or T opposite a 6-methyl-guanine, with respect to the correct C. This is the first example of an alternative proofreading mechanism used during TLS.

DOI: https://doi.org/10.1038/embor.2011.226

EMBO reports

scientific report

A new proofreading mechanism for lesion bypass by DNA polymerase-λ

Emmanuele Crespan[1,2], *Giovanni Maga*[1*+] & *Ulrich Hübscher*[2*]

[1]Institute of Molecular Genetics IGM-CNR, Pavia, Italy, and [2]Institute for Veterinary Biochemistry and Molecular Biology, University of Zürich-Irchel, Zürich, Switzerland

Replicative DNA polymerases (DNA pols) increase their fidelity by removing misincorporated nucleotides with their 3′→5′ exonuclease activity. Exonuclease activity reduces translesion synthesis (TLS) efficiency and TLS DNA pols lack 3′→5′ exonuclease activity. Here we show that physiological concentrations of pyrophosphate (PP_i) activate the pyrophosphorolytic activity by DNA pol-λ, allowing the preferential excision of the incorrectly incorporated A opposite a 7,8-dihydro-8-oxoguanine lesion, or T opposite a 6-methyl-guanine, with respect to the correct C. This is the first example of an alternative proofreading mechanism used during TLS.

Keywords: DNA repair; translesion synthesis; fidelity; proofreading; pyrophosphorolysis

EMBO *reports* (2012) **13**, 68–74. doi:10.1038/embor.2011.226

INTRODUCTION

The frequent oxidative DNA damage, 7,8-dihydro-8-oxoguanine (8-oxo-G), induces erroneous DNA replication and A/8-oxo-G mismatch formation in living cells (Brieba *et al*, 2004; Freisinger *et al*, 2004; Hsu *et al*, 2004). Sanitization of newly replicated DNA by base excision repair (BER) absolutely requires the error-free bypass of the 8-oxo-G lesion by a specialized DNA polymerase (DNA pol; van Loon & Hubscher, 2009). Previous work from our laboratory has identified DNA pol-λ as the key enzyme in this process, as it incorporated C opposite 8-oxo-G, 100-fold better than the incorrect A, together with the two auxiliary proteins proliferating-cell nuclear antigen and RP-A (Maga *et al*, 2007, 2008). Because of this essential role, it is important to understand the mechanisms accounting for the fidelity of DNA pol-λ on this lesion, with respect to the closely related DNA pol-β (Werneburg *et al*, 1996; Garcia-Diaz *et al*, 2005a, b; Beard & Wilson, 2006; Moon *et al*, 2007). Replicative DNA pols increase their intrinsic fidelity through their 3′→5′ exonuclease proofreading activity that removes misincorporated nucleotides (Echols & Goodman, 1991; Kunkel & Bebenek, 2000). Both DNA pols-λ and -β lack exonuclease activities, but their intrinsic fidelity ($\sim 10^{-5}$) is enough to ensure faithful copying of the short tract (1–9 nt) of undamaged DNA required in BER. The repair of A/8-oxo-G mismatches, however, poses a unique problem, as it has to reconcile the seemingly opposite features of high fidelity and efficient translesion synthesis (TLS). The efficiency of TLS synthesis depends on the ability of specialized DNA pols to incorporate a nucleotide opposite a damaged base on the template and to elongate it efficiently (Beard & Wilson, 2001; Friedberg *et al*, 2001; Prakash *et al*, 2005). As distorted primer ends are likely to be targeted by the 3′→5′ proofreading exonuclease, such an activity is incompatible with TLS, and exonuclease-proficient DNA pols are less efficient in lesion bypass than exonuclease-deficient enzymes (Khare & Eckert, 2002; Prakash *et al*, 2005), raising the question of whether other mechanisms exist for fidelity enhancement during TLS.

It has been shown that the HIV-1 reverse transcriptase and *Sulfolobus solfataricus* Dpo4 DNA pol can efficiently remove the last incorporated nucleotide by a phosphorolytic mechanism, using inorganic pyrophosphate (PP_i; Goldschmidt & Marquet, 2004; Vaisman *et al*, 2005). Such an activity, however, has never been shown for any animal cell DNA pol.

Here we show that DNA pol-λ has the unique ability to preferentially remove incorrectly incorporated A or T opposite 8-oxo-G and 6-methyl guanine lesions, respectively, with respect to the correct C, and that it does this through a pyrophosphorolytic activity at physiological concentrations of PP_i. This is the first example of an alternative proofreading mechanism used during TLS.

RESULTS

Pyrophosphorolysis by human DNA polymerases

Even in the presence of millimolar concentrations of PP_i or the four ribonucleotide triphosphates, neither the family X enzymes DNA pol-λ, -β, -μ, and terminal transferase (TdT) nor the replicative family B DNA pol-α could remove a 3′-mismatched nucleotide from a DNA primer/template through phosphorolysis (data not shown).

On the other hand, using a primer/template with a correct terminal base pairing, the four family X DNA pols and the family B

[1]Institute of Molecular Genetics IGM-CNR, via Abbiategrasso 207, I-27100 Pavia, Italy
[2]Institute for Veterinary Biochemistry and Molecular Biology, University of Zürich-Irchel, Winterthurerstrasse 190, CH-8057 Zürich, Switzerland
*These authors share senior authorship
+Corresponding author. Tel: +39 0382 564354; Fax: +39 0382 422286; E-mail: maga@igm.cnr.it

Received 16 August 2011; revised 12 October 2011; accepted 12 October 2011; published online 2 December 2011

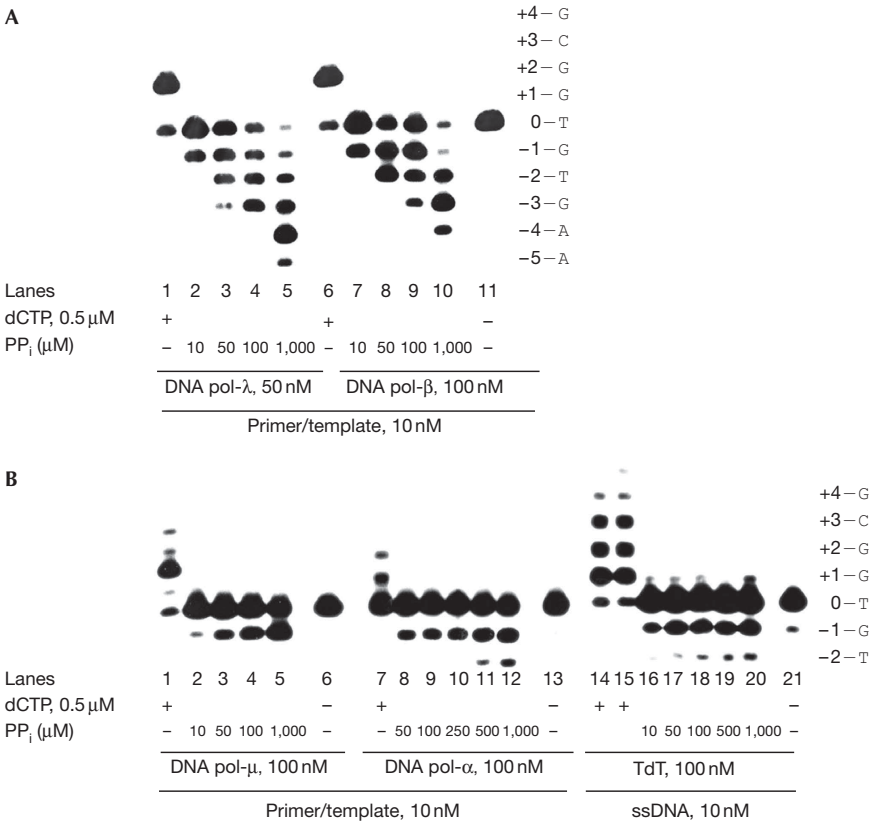

Fig 1 | All four family X DNA polymerases and the exonuclease-deficient DNA pol-α contain pyrophosphorolytic activity. (**A**) Pyrophosphorolytic activity of DNA polymerase (DNA pol)-λ (lanes 2–5) and DNA pol-β (lanes 7–10). Lanes 1 and 6: DNA synthesis reactions in the presence of deoxycytidine triphosphate (dCTP). Lane 11: control reaction in the absence of pyrophosphate (PP_i) or nucleotides. The sequence corresponding to positions −5 to +4 of the template strand is indicated at the right. (**B**) Pyrophosphorolytic activity of DNA pol-μ (lanes 2–5), DNA pol-α (lanes 8–12) and terminal transferase (TdT; lanes 16–20). Lanes 6, 13 and 21: control reactions in the absence of PP_i or nucleotides. Lanes 1, 7, 14 and 15: DNA synthesis reaction in the presence of dCTP. Each reaction was incubated for 5 min. ssDNA, single-stranded DNA.

DNA pol-α were able to remove, although with different efficiencies, the last 3′-terminal nucleotides in the presence of PP_i (Fig 1), but not ribonucleotide triphosphates (data not shown). DNA pols-λ and -β showed the highest pyrophosphorolysis activity, being able to remove several nucleotides consecutively, with K_m values for PP_i of 50 and 111 μM, respectively (Fig 1A), whereas DNA pol-μ and DNA pol-α showed a limited ability to perform pyrophosphorolysis (Fig 1B). TdT was able to perform a pyrophosphorolytic reaction on its preferred template single-stranded DNA (Fig 1B, lanes 16–20), whereas DNA pol-λ and DNA pol-μ were not able to perform pyrophosphorolysis on a single-stranded DNA, even at millimolar concentration of PP_i (data not shown).

Pyrophosphorolysis of dA paired to 8-oxoG

To directly visualize the PP_i-dependent formation of nucleoside triphosphates, a 5′-fluorescently labelled DNA substrate with a terminal C:8-oxo-G base pair was incubated in the presence of DNA pol-λ and ^{32}P-PP_i. Pyrophosphorolytic degradation was visualized by gel analysis (supplementary Fig S1A online), whereas the newly formed ^{32}P-deoxycytidine triphosphate (dCTP) was visualized by thin-layer chromatography (supplementary Fig S1B online). These data clearly indicated that the observed primer degradation was mediated by pyrophosphorolysis. We next tested whether the pyrophosphorolytic activity could further enhance the ability of DNA pol-λ to discriminate between the correct (C) and incorrect (A) base pairing opposite an 8-oxo-G (Maga *et al*, 2007). In the presence of PP_i, DNA pol-λ was able to promote pyrophosphorolysis with a primer/template in which the last nucleotide paired with an 8-oxo-G on the template strand was either A or C, but with different efficiencies. The V_{max}/K_m ratio was higher for the A/8-oxo-G base pairing than for C/8-oxo-G. When tested on the same substrates, DNA pol-β showed eightfold lower pyrophosphorolytic activity when an A was paired with 8-oxo-G than when a C was present opposite the lesion (Fig 2A,B; supplementary Table S1 online).

DNA polymerase-λ phosphorolysis on nicked DNA

We next investigated the ability of DNA pols-β and -λ to catalyse pyrophosphorolysis on nicked substrates containing an 8-oxo-G lesion paired with A or C, mimicking the post-incorporation product of an error-prone or error-free gap-filling reaction, respectively, generated by BER reactions dependent on the removal by the MUTYH glycosylase of an A:8-oxo-G mispair (van Loon and Hubscher, 2009). A nicked DNA substrate bearing a normal C/G base pair was used as a control. Both DNA pols

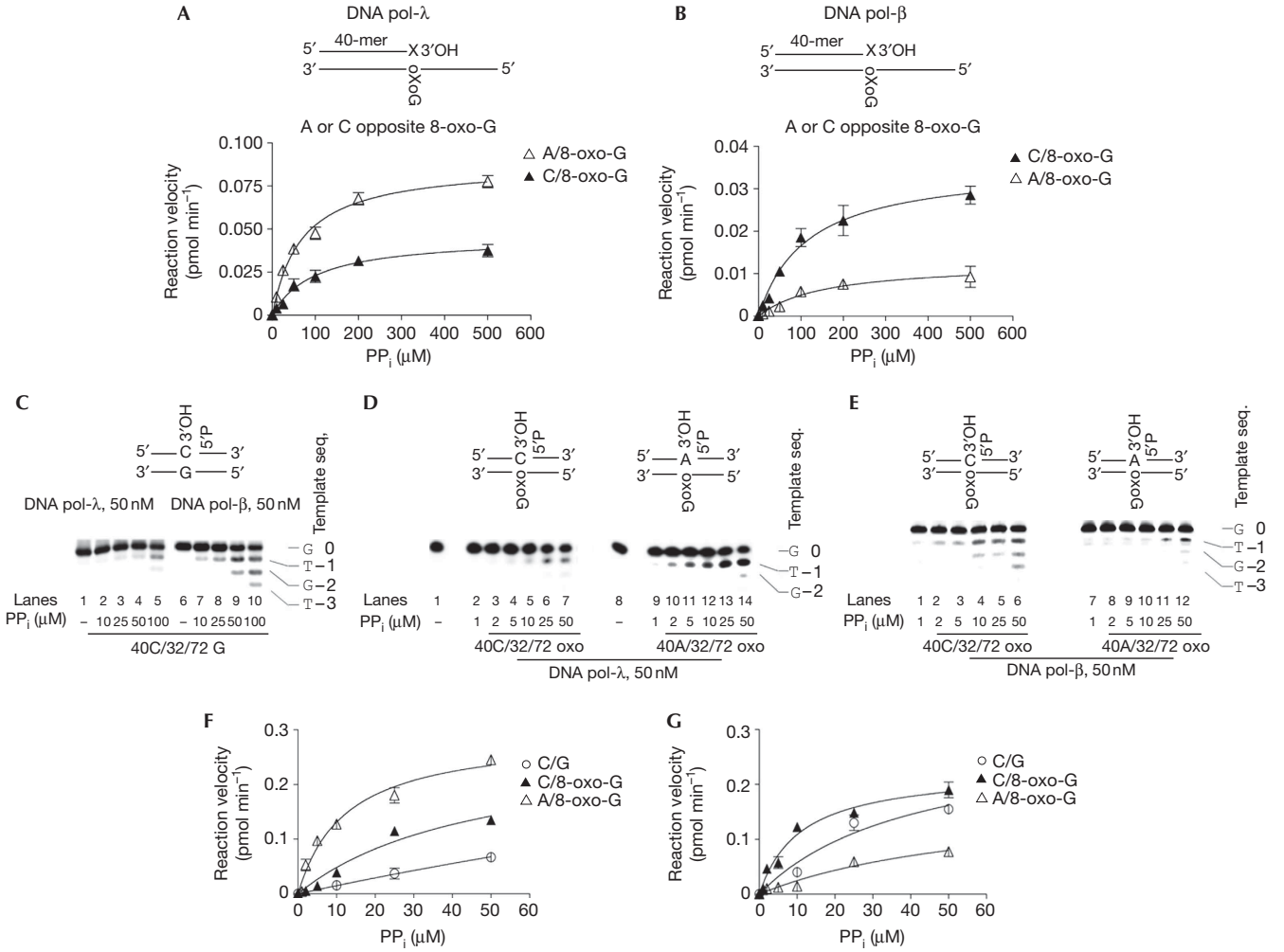

Fig 2 | DNA polymerase-λ, but not DNA polymerase-β, showed enhanced pyrophosphorolytic activity on dA paired to 8-oxo-G. All reactions were performed for 5 min with 50 nM primer/template A/7,8-dihydro-8-oxoguanine (8-oxo-G) or C/8-oxo-G and 50 nM of DNA polymerase (DNA pol)-λ or DNA pol-β. (**A**) Variation of the velocity (pmols of nucleotide removed) of the pyrophosphorolytic reaction by DNA pol-λ as a function of the pyrophosphate (PP_i) concentration, in the presence of A/8-oxo-G (empty triangles) or C/8-oxo-G (filled triangles) terminal base pairs. Values are the mean of three independent experiments. Error bars are ± s.d. (**B**) As in (**A**), but in the presence of DNA pol-β. (**C**) DNA pol-λ (lanes 1–5) and -β (lanes 6–10) in the presence of nicked DNA substrates with C/G-terminal base pairs at the 3′-side of the nick, in the presence of different PP_i concentrations (10–100 μM). Lanes 1 and 6: control reactions in the absence of PP_i. (**D**) DNA pol-λ in the presence of nicked DNA substrates with a C/8-oxo-G (lanes 1–7) or A/8-oxo-G (lanes 8–14) terminal base pairs at the 3′-side of the nick, in the presence of different PP_i concentrations (1–50 μM). Lanes 1 and 8: control reactions in the absence of PP_i. (**E**) As in (**D**), but with DNA pol-β. (**F**) Variations of the velocity (pmols of nucleotide removed) of the pyrophosphorolytic reaction by DNA pol-λ on C/G (circles), C/8-oxo-G (filled triangles) or A/8-oxo-G (empty triangles)-nicked DNA templates, as a function of PP_i concentrations. Values are the mean of three independent experiments. Error bars are ± s.d. (**G**) As in (**F**), but with DNA pol-β. All the reactions were incubated for 5 min with 50 nM nicked DNA substrates.

were able to perform pyrophosphorolysis on these substrates (Fig 2C–E). The catalytic efficiency of DNA pol-β was enhanced on this substrate with both A/oxo-G and C/oxo-G base pairs (Supplementary Table S2 online); in fact, removal of the nucleotide opposite 8-oxo-G would create a 1-nt gap, which is the preferred substrate for DNA pol-β. DNA pol-λ removed a wrong A opposite 8-oxo-G with a 10-fold higher efficiency (V_{max}/K_m values) than a correct C, whereas DNA pol-β pyrophosphorolytic efficiency on this nicked substrate was reduced fivefold containing an A/8-oxo-G pair, with respect to C/8-oxo-G (Fig 2F,G; supplementary Table S2 online). As a result, DNA pol-λ was 12-fold more efficient than DNA pol-β in removing A opposite 8-oxo-G.

To directly show that this difference also reflected a different pyrophosphorolysis-dependent synthesis of dNTPs, production of radioactive dATP or dCTP starting from ^{32}P-PP_i was monitored in the presence of nicked substrates, containing either an A/8-oxo-G or a C/8-oxo-G base pair. As shown in Fig 3A, time-dependent

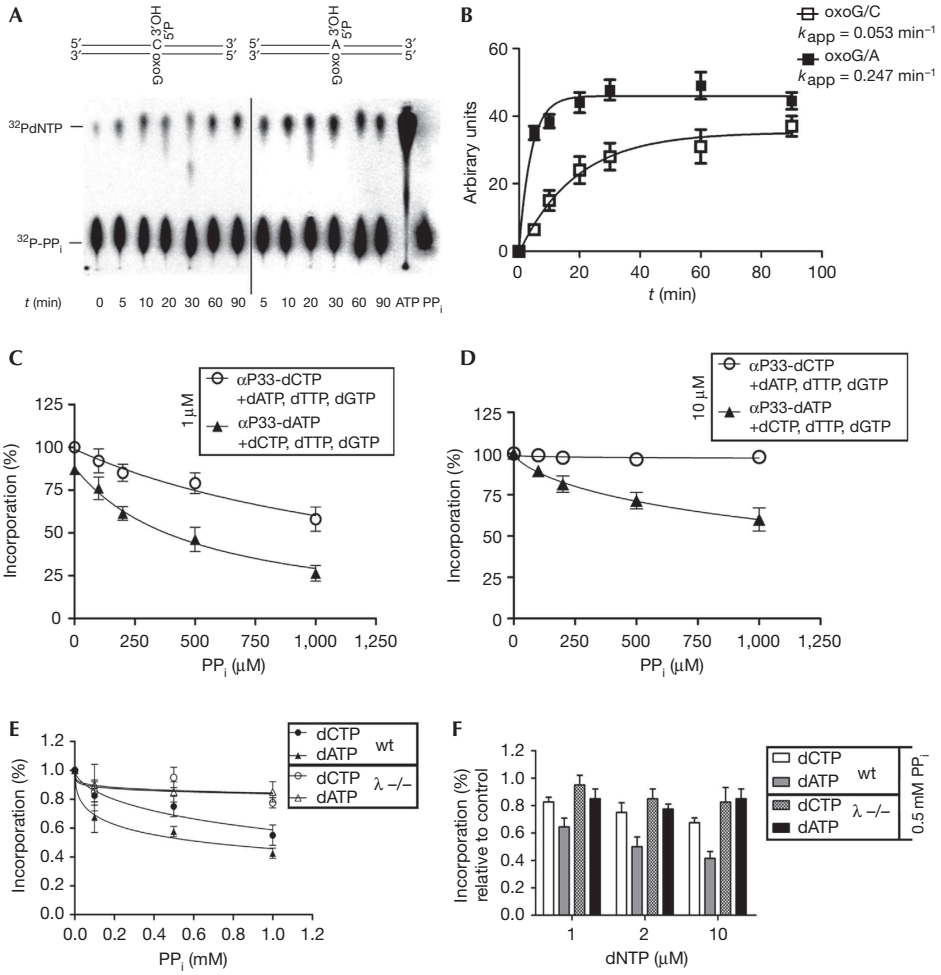

Fig 3 | DNA polymerase-λ shows preferential pyrophosphorolytic removal of an A/8-oxo-G base pair on nicked DNA substrates. (**A**) Time course for the pyrophosphorolysis-dependent formation of radioactive dNTP by DNA polymerase (DNA pol)-λ, starting from ^{32}P-pyrophosphate (PP_i) as the precursor, in the presence of nicked DNA templates with a C/7,8-dihydro-8-oxoguanine (8-oxo-G; lanes 1–7) or A/8-oxo-G (lanes 8–13) base pair. All reactions were performed in parallel starting from a single mix, and the products were separated together on a single TLC plate. The t_0 time point is common to both reaction mixtures. Lane 14: radioactive dATP. Lane 15: radioactive PP_i. (**B**) Single-exponential curves for time-dependent accumulation of radioactive dNTPs, under the conditions shown in (**A**). Values are expressed as arbitrary intensity units and are the means of three independent experiments. Error bars represent ± s.d. (**C**) PP_i-dependent inhibition of radioactive deoxycytidine triphosphate (αP33-dCTP circles) or deoxyadenosine triphosphate (αP33dATP, triangles) incorporation, opposite 8-oxo-G on a 1-nt gap template, in the presence of all four dNTPs at 1 μM final concentration. Values are the means of three independent experiments. Error bars represent ± s.d. (**D**) As in (**C**), but at a final dNTPs concentration of 10 μM. (**E**) PP_i-dependent inhibition of dCTP (circles) or dATP (triangles) incorporation opposite 8-oxo-G in wild-type (wt, filled symbols) or $\lambda^{-/-}$ (empty symbols) mouse embryonic fibroblast (MEF) extracts. (**F**) Relative incorporation opposite 8-oxo-G by wt and $\lambda^{-/-}$ MEF extracts, in the presence of aphidicolin (10 μg ml^{-1}), 0.5 mM PP_i and three different concentrations of dATP or dCTP.

formation of radioactive nucleotide triphosphate was higher in the presence of an A/8-oxo-G pair (lanes 8–13) than with a C/8-oxo-G (lanes 2–7). The apparent rates for nucleotide formation were 0.053 ± 0.001 min^{-1} with C/8-oxo-G and 0.247 ± 0.005 min^{-1} with A/8-oxo-G, respectively (Fig 3B). Thus, on a nicked template, A opposite an 8-oxo-G was removed faster than C by the pyrophosphorolytic activity of DNA pol-λ.

Pyrophosphate increases the fidelity of lesion bypass

To test whether PP_i could enhance the overall fidelity of DNA pol-λ in the bypass of an 8-oxo-G, nucleotide incorporation opposite an 8-oxo-G lesion was assayed at increasing concentrations of dATP or dCTP in the presence of 0, 50 and 100 μM PP_i (supplementary Fig S1C,D online). The ratio between the nucleotide incorporation specificity of DNA pol-λ (k_{cat}/K_m values) for dCTP and dATP, respectively (indicated as dC/dA in supplementary Table S3 online), in the absence of PP_i was 3.7. This ratio increased to 7.4 when PP_i was present at 100 μM concentration, suggesting that PP_i enhanced the fidelity of 8-oxo-G bypass by DNA pol-λ. To directly monitor the effects of PP_i on the incorporation of either dATP or dCTP opposite an 8-oxo-G, a mixture of all four dNTPs, in which either ^{33}P-dATP or ^{33}P-dCTP

were added in equimolar amount, was used. Nucleotide incorporation on a 1-nt gapped DNA template with an 8-oxo-G lesion was measured in the absence or presence of increasing PP_i concentrations. Two dNTPs concentrations close to the physiological levels of dNTPs in resting versus proliferating cells were used, which fall either close to (1 μM) or above (10 μM) the K_m of DNA pol-λ for dCTP. At a final dNTPs concentration of 1 μM, PP_i inhibited dATP incorporation 2.5-fold more efficiently than dCTP (Fig 3C; supplementary Fig S1E online). When the dNTPs concentration was raised to 10 μM, dCTP incorporation was unaffected by PP_i, whereas dATP incorporation was still reduced 1.7-fold (Fig 3D; supplementary Fig S1F online). When either dATP or dCTP were maintained at limiting concentrations, in the presence of 10 μM dTTP and dGTP, PP_i inhibited dATP incorporation opposite 8-oxo-G 2.5-fold more than dCTP incorporation (supplementary Fig S1G,H online). Incorporation of a second nucleotide was lower in the case of an A/8-oxo-G base pair (supplementary Fig S1F online), reflecting the slow elongation rate of A/8-oxo-G-terminated primers by DNA pol-λ (Picher and Blanco, 2007). However, on a 1-nt gapped substrate with a different sequence context, where no elongation of C/oxo-G or A/oxo-G base pairs could occur (supplementary Fig S2A,B online), PP_i was still able to inhibit the incorporation of dATP opposite 8-oxo-G more than dCTP. Furthermore, time course experiments demonstrated that PP_i could reduce the apparent rate of dATP incorporation opposite the lesion threefold more than in the case of dCTP, in the absence of A/oxo-G primer elongation (supplementary Fig S2C–F online).

Finally, PP_i could also enhance faithful TLS by DNA pol-λ on the very mutagenic 6-methylguanine (6-mG). Similarly to other DNA pols, DNA pol-λ bypasses this lesion in a mutagenic manner, incorporating T with nearly the same efficiency as C. As shown in supplementary Table S3 online, PP_i enhanced about fourfold the fidelity of TLS by DNA pol-λ on this lesion, too, by preferentially inhibiting incorporation of the incorrect T versus the correct C.

Cell extracts from *POLL*$^{+/+}$ (wild type) and *POLL*$^{-/-}$ mouse embryonic fibroblasts were tested for 8-oxo-G bypass in the presence of aphidicolin (to inhibit the three replicative DNA pols-α, -δ and -ε) and either dCTP or dATP, and in the absence or presence of increasing concentrations of PP_i. As shown in Fig 3E, PP_i inhibited dATP incorporation more effectively than dCTP incorporation, opposite 8-oxo-G, but in *POLL*$^{+/+}$ extracts only, whereas in the absence of endogenous DNA pol-λ PP_i had no effect. Similarly, when increasing amounts of dCTP or dATP were titrated into the reaction, in the absence or presence of a fixed dose of PP_i, the relative incorporation of dATP was lower than that of dCTP, but only in wild-type extracts, whereas in the absence of endogenous DNA pol-λ no significant differences were noted (Fig 3F). The difference between dATP and dCTP relative incorporation was lower than the one observed with purified enzymes, because of the presence of several DNA pols in the extracts, preferentially incorporating dATP opposite the lesion, but unable to remove it by pyrophosphorolysis. These data indicated that DNA pol-λ is the main cellular enzymatic activity using pyrophosphorolysis as a general new proofreading mechanism for TLS over 8-oxo-G and 6-mG.

DISCUSSION

This study shows that PP_i can function as a cofactor enhancing the fidelity of 8-oxo-G and 6-mG bypass by DNA pol-λ. Neither proliferating-cell nuclear antigen nor RP-A showed any effect on the DNA pol-λ pyrophosphorolysis reaction (data not shown), consistent with their proposed role at the level of incorporation, but not at the post-incorporation step, during lesion bypass (Maga *et al*, 2008).

Pyrophosphorolysis has been originally suggested as a possible mechanism for fidelity (Lecomte *et al*, 1986), and phosphorolytic primer degradation has been shown to increase fidelity of HIV-1 reverse transcriptase and Dpo4 (Goldschmidt & Marquet, 2004; Vaisman *et al*, 2005). Thus, DNA pol-λ is the first example of a human DNA pol using pyrophosphorolysis to achieve higher fidelity at physiological intracellular PP_i concentrations (measured in the 10–100 μM range, depending on the cellular proliferative state; Lust & Seegmiller, 1976; Yamada *et al*, 1988; Barshop *et al*, 1991). The K_m for the PP_i-dependent dAMP removal opposite 8-oxo-G by DNA pol-λ (12 μM) falls within the estimated intracellular PP_i level in non-proliferating cells (10 μM). In contrast, the K_m for dCMP removal under similar conditions was found to be >100 μM, making it unlikely that PP_i would catalyse removal of the correct C paired to an 8-oxo-G lesion under normal conditions. DNA pol-β showed a K_m value of 75 μM for its PP_i-dependent removal of dAMP on nicked templates, suggesting that pyrophosphorolysis is probably not contributing to its selectivity under physiological conditions. Structural and molecular studies (Garcia-Diaz *et al*, 2005b; Fowler *et al*, 2009) showed that residues R386 and R420 of DNA pol-λ stabilize the leaving PP_i. Among family X enzymes, only DNA pol-β bears both equivalent residues (R149 and R183); DNA pol-μ and TdT have only one (R323 and R336, respectively). This correlates with our observation that DNA pols-β and -λ are the most proficient in pyrophosphorolysis among family X enzymes. DNA pol-λ has high affinity for dNTPs (>30-fold over pol-β), suggesting its possible involvement in DNA transactions occurring under low cellular levels of dNTPs (Garcia-Diaz *et al*, 2002). Indeed, we showed that DNA pol-λ could remove dATP opposite 8-oxo-G more efficiently than dATP, at both saturating (10 μM) and limiting (1 μM) dNTP concentrations. Selectivity for nucleotide incorporation by TLS DNA pols is not dictated by the identity of a normal templating base, but rather by the identity of the templating lesion (Prakash *et al*, 2005). Thus, proofreading by pyrophosphorolysis during TLS requires a mechanism to ensure that hydrolysis is taking place only in the event of 'incorrect' nucleotide incorporation. Two conditions are to be met: first, that the enzyme should have a relatively high affinity for PP_i, and second, that a difference should exist in the rate of catalysis between the 'correct' incorporation event and the one that needs proofreading. DNA pol-λ satisfies both these criteria: it has high affinity for PP_i and it shows lower incorporation rates of dATP opposite 8-oxo-G, with respect to dCTP, and lower elongation efficiency of A/8-oxo-G base pairs, with respect to C/8-oxo-G ones. Thus, in the event of dAMP incorporation opposite 8-oxo-G, the combination of slow PP_i dissociation and slow translocation/elongation rates would allow PP_i to stay in the active site, ensuring pyrophosphorolytic degradation of A/oxo-G base pairs only (supplementary Fig S2G online).

According to this model, one might predict that DNA pol-λ should be capable of PP_i-dependent proofreading on template lesions that are slowing its catalytic rate. We have directly demonstrated this in the case of the 6-mG lesion. DNA pol-λ can

incorporate T opposite this lesion, but at a slower rate than C. Addition of PP_i significantly reduced T, but not C, incorporation (supplementary Table S3 online).

In summary, we propose that, besides specialized DNA pols and auxiliary factors, cells also evolved a specialized proofreading mechanism to ensure high bypass accuracy of certain lesions, such as 8-oxo-G and 6-mG.

METHODS

***In vitro* DNA synthesis and pyrophosphorolysis reactions.** For denaturing gel analysis of DNA synthesis and pyrophosphorolysis products, the reaction mixtures (10 μl) contained 50 mM Tris–HCl (pH 7.0), 0.25 mg ml^{-1} BSA, 1 mM dithiothreitol and 1 mM Mg^{2+}. Concentrations of purified DNA pols-α, -β, -λ, -μ and TdT (Weiser *et al*, 1991; Ramadan *et al*, 2004), dNTPs and the 5′ ^{32}P-labelled primer/template were as indicated in the figure legends. Reactions were incubated for 5 min at 37 °C and then stopped by the addition of standard denaturing gel loading buffer (95% formamide, 10 mM EDTA, xylene cyanol, and bromophenol blue), heated at 95 °C for 5 min and loaded on a 7 M urea/12% polyacrylamide gel. Reactions including [α-^{33}P]dATP or [α-^{33}P]dCTP were performed under the same conditions, but in the presence of equimolar amounts of the three unlabelled dNTPs and with a 5′-unlabelled primer/template.

A volume of 4 μl of the reactions including ^{32}P-PP_i were spotted on a polyethyleneimine cellulose thin layer chromatography plate and developed in 4 M Na-formate, pH 3.4. Position of the ^{32}P-PP_i and ^{32}P-dCTP was detected by PhosphorImager (Typhoon Trio; GE Healthcare). Reactions with mouse embryonic fibroblast extracts were performed under the same conditions in the presence of 1 μg (total proteins) of extracts and 10 μg ml^{-1} aphidicolin.

Steady-state kinetic analysis. Reactions were performed as described above. Quantification was done by scanning densitometry with a PhosphorImager (Typhoon Trio; GE Healthcare). Incubation time was determined by preliminary time course experiments to satisfy the requirements for initial velocity (linearity and substrate utilization $\leqslant$30%). The initial velocities of the reaction were calculated (Image Quant and GraphPad Prism 3.0) from the values of integrated gel band intensities.

Quantification of the pyrophosphorolytic reactions was performed from the values of integrated gel band intensities:

$$\sum IT_{(-1,-n)} / \sum IT$$

where T is the target site, the template position of interest; $\sum IT$ is the sum of the integrated intensities at positions T, $T-1,\ldots,$ $T-n$; and $\sum IT_{(-1,\ -n)}$ is the sum of the integrated intensities at positions $T-1,\ldots,$ $T-n$.

The apparent K_m and k_{cat} values were calculated by plotting the initial velocities against the nucleotide, PP_i or primer substrate concentrations and fitting the data according to the Michaelis–Menten equation:

$$k_{cat}[E]_0/(1 + K_m/[S]),$$

where $[E]_0$ is the input enzyme concentration and [S] is the variable substrate. Substrate incorporation efficiencies, as well as pyrophosphorolytic nucleotide removal, were defined as the k_{cat}/K_m ratio.

Supplementary information is available at EMBO *reports* online (http://www.emboreports.org).

ACKNOWLEDGEMENTS

This work was supported by the Swiss National Science Foundation (grant 3100-109312/2) and the UBS 'Im Auftrag eines Kunden' to E.C. and U.H., and by the University of Zurich to U.H. and in part to G.M., and by the Italian Association for Cancer Research AIRC IG4538 and the Superpig Program, project cofinanced by Lombardy Region through the 'Fund for promoting institutional agreements', to G.M. E.C. was also supported by an Italian Foundation for Cancer Research Fellowship.

CONFLICT OF INTEREST

The authors declare that they have no conflict of interest.

REFERENCES

Barshop BA, Adamson DT, Vellom DC, Rosen F, Epstein BL, Seegmiller JE (1991) Luminescent immobilized enzyme test systems for inorganic pyrophosphate: assays using firefly luciferase and nicotinamide-mononucleotide adenylyl transferase or adenosine-5′-triphosphate sulfurylase. *Anal Biochem* **197:** 266–272

Beard WA, Wilson SH (2001) DNA lesion bypass polymerases open up. *Structure* **9:** 759–764

Beard WA, Wilson SH (2006) Structure and mechanism of DNA polymerase β. *Chem Rev* **106:** 361–382

Brieba LG, Eichman BF, Kokoska RJ, Doublie S, Kunkel TA, Ellenberger T (2004) Structural basis for the dual coding potential of 8-oxoguanosine by a high-fidelity DNA polymerase. *EMBO J* **23:** 3452–3461

Echols H, Goodman MF (1991) Fidelity mechanisms in DNA replication. *Annu Rev Biochem* **60:** 477–511

Freisinger E, Grollman AP, Miller H, Kisker C (2004) Lesion (in)tolerance reveals insights into DNA replication fidelity. *EMBO J* **23:** 1494–1505

Fowler JD, Brown JA, Kvaratskhelia M, Suo Z (2009) Probing conformational changes of human DNA polymerase lambda using mass spectrometry-based protein footprinting. *J Mol Biol* **390:** 368–379

Friedberg EC, Fischhaber PL, Kisker C (2001) Error-prone DNA polymerases: novel structures and the benefits of infidelity. *Cell* **107:** 9–12

Garcia-Diaz M *et al* (2002) DNA polymerase λ, a novel DNA repair enzyme in human cells. *J Biol Chem* **277:** 13184–13191

Garcia-Diaz M, Bebenek K, Gao G, Pedersen LC, London RE, Kunkel TA (2005a) Structure–function studies of DNA polymerase λ. *DNA Repair (Amst)* **4:** 1358–1367

Garcia-Diaz M, Bebenek K, Krahn JM, Kunkel TA, Pedersen LC (2005b) A closed conformation for the Pol λ catalytic cycle. *Nat Struct Mol Biol* **12:** 97–98

Goldschmidt V, Marquet R (2004) Primer unblocking by HIV-1 reverse transcriptase and resistance to nucleoside RT inhibitors (NRTIs). *Int J Biochem Cell Biol* **36:** 1687–1705

Hsu GW, Ober M, Carell T, Beese LS (2004) Error-prone replication of oxidatively damaged DNA by a high-fidelity DNA polymerase. *Nature* **431:** 217–221

Khare V, Eckert KA (2002) The proofreading 3′→5′ exonuclease activity of DNA polymerases: a kinetic barrier to translesion DNA synthesis. *Mutat Res* **510:** 45–54

Kunkel TA, Bebenek K (2000) DNA replication fidelity. *Annu Rev Biochem* **69:** 497–529

Lecomte P, Doubleday OP, Radman M (1986) Evidence for an intermediate in DNA synthesis involving pyrophosphate exchange. A possible role in fidelity. *J Mol Biol* **189:** 643–652

Lust G, Seegmiller JE (1976) A rapid, enzymatic assay for measurement of inorganic pyrophosphate in biological samples. *Clin Chim Acta* **66:** 241–249

Maga G, Villani G, Crespan E, Wimmer U, Ferrari E, Bertocci B, Hubscher U (2007) 8-oxo-guanine bypass by human DNA polymerases in the presence of auxiliary proteins. *Nature* **447:** 606–608

Maga G *et al* (2008) Replication protein A and proliferating cell nuclear antigen coordinate DNA polymerase selection in 8-oxo-guanine repair. *Proc Natl Acad Sci USA* **105:** 20689–20694

Moon AF, Garcia-Diaz M, Batra VK, Beard WA, Bebenek K, Kunkel TA, Wilson SH, Pedersen LC (2007) The X family portrait: structural insights into biological functions of X family polymerases. *DNA Repair (Amst)* **6:** 1709–1725

Picher AJ, Blanco L (2007) Human DNA polymerase λ is a proficient extender of primer ends paired to 7,8-dihydro-8-oxoguanine. *DNA Repair (Amst)* **6:** 1749–1756

Prakash S, Johnson RE, Prakash L (2005) Eukaryotic translesion synthesis DNA polymerases: specificity of structure and function. *Annu Rev Biochem* **74:** 317–353

Ramadan K, Shevelev IV, Maga G, Hubscher U (2004) *De novo* DNA synthesis by human DNA polymerase λ, DNA polymerase μ and terminal deoxyribonucleotidyl transferase. *J Mol Biol* **339:** 395–404

van Loon B, Hubscher U (2009) An 8-oxo-guanine repair pathway coordinated by MUTYH glycosylase and DNA polymerase λ. *Proc Natl Acad Sci USA* **106:** 18201–18206

Vaisman A, Ling H, Woodgate R, Yang W (2005) Fidelity of Dpo4: effect of metal ions, nucleotide selection and pyrophosphorolysis. *EMBO J* **24:** 2957–2967

Weiser T, Gassmann M, Thommes P, Ferrari E, Hafkemeyer P, Hubscher U (1991) Biochemical and functional comparison of DNA polymerases α, δ, and ε from calf thymus. *J Biol Chem* **266:** 10420–10428

Werneburg BG, Ahn J, Zhong X, Hondal RJ, Kraynov VS, Tsai MD (1996) DNA polymerase β: pre-steady-state kinetic analysis and roles of arginine-283 in catalysis and fidelity. *Biochemistry* **35:** 7041–7050

Yamada T, Inoue T, Nishida T, Furuya E, Tagawa K (1988) Hepatic accumulation of pyrophosphate during acetate metabolism. *J Biochem* **104:** 847–850